Analysis of seismic behaviour of an offshore wind turbine with a flexible foundation

Yang Yang [a,b], Musa Bashir [b], Chun Li [a,*], Jin Wang [b]

[a] School of Energy and Power Engineering, University of Shanghai for Science and Technology, Shanghai, 200093, P.R. China

[b] Department of Maritime and Mechanical Engineering, Liverpool John Moores University, Liverpool, Byrom Street, L3 3AF, UK

Abstract: This paper investigates the effects of nonlinear soil behaviours on the structural responses of offshore wind turbines (OWTs) subjected to wind, wave and earthquake loadings. A novel seismic analysis framework (SAF) is developed for the assessment of seismic behaviours of OWTs with flexible and fixed foundations. The SAF consists of an improved QuakeDyn module that is implemented into an open source tool (FAST). SAF has been validated through benchmark studies using numerical tools and the results show good agreements. Fully coupled nonlinear simulations have been performed for OWTs with fixed and flexible foundations under operational, parked and emergency shutdown states. The flexible foundation is modelled using nonlinear *p-y* curves obtained using LPILE. For all the examined operating conditions, notable differences of magnitude and variation in the responses between the flexible and fixed cases are observed, indicating the need for soil effects to be accounted in seismic behaviour analysis of wind turbines. It is further observed that the earthquake induces more severe vibrations on wind turbines with a flexible foundation compared to the one with a fixed base. Also, aerodynamic damping dissipates more energy from earthquake excitation resulting in a smaller tower-top fore-aft displacement. The shutdown triggered by the earthquake causes a 34% increase in the mudline bending moment for the flexible foundation case, while a decreasing trend is observed for the fixed foundation model. Similar observations are made

* Corresponding author: lichun_usst@163.com

regarding the tower-top displacements. The observations imply that ignoring the soil effect may lead to misjudgement of the consequence of an emergency shutdown. The relative orientation of the ground motion with respect to the wind direction causes significant difference in the seismic behaviour of the wind turbine. This confirms that it is necessary to interchange the horizontal components of an earthquake in order to consider the intersectional effect between ground motion and wind.

Keywords: Offshore Wind Turbine; Dynamic Behaviour; Seismic Assessment; Nonlinear Soil Effect.

1 Introduction

As the demand for additional sources of cleaner energy continue to increase in order to meet the constantly increasing global energy consumption, renewable sourced power has become the energy source of choice due to environmental concerns. In particular, wind energy has a comparatively low-cost process for increasing power generation around the world. Newly installed capacity in 2016 has contributed over 10% to the total cumulative installations of 500 GW [1], and 23.4% of this installed capacity was added in China. Most of these new installations are found along the earthquake prone areas of north-western and south-eastern coasts of China. Wind turbines installed in these locations are expected to be susceptible to damage caused by earthquake events. Similar circumstances exist for the wind farms located along the west coast of United States, Southern areas of European and New Zealand where there are rich offshore wind resources as shown in Fig. 1 [2]. It is therefore imperative to analyse the response of OWTs subjected to the combined effects of hazards associated with wind, wave and earthquake.

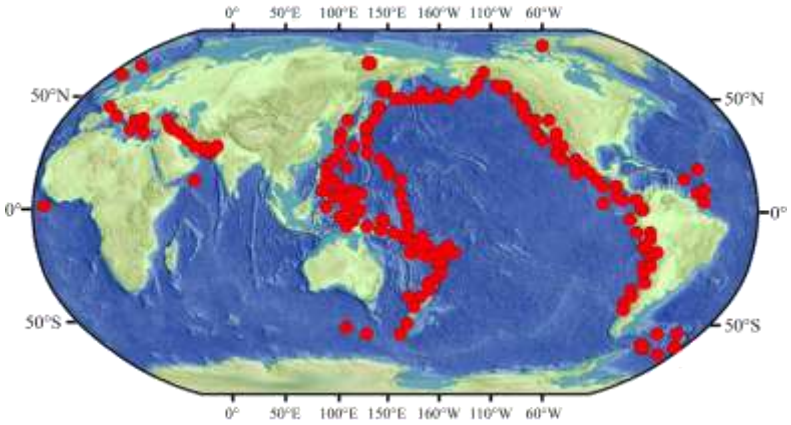

Fig.1: Global distribution for the more than 300 earthquake events with Richter magnitude values over 6 during 2007~2016.

Analysis of seismic effects in the design of OWT is commonly performed using the Response Spectral Method (RSM). The method has been widely used to estimate seismic loading demand in the frequency domain for wind turbines [3-5]. Seismic loading demands are estimated based on modal analysis concept for a given response spectrum. The effects of damping due to aerodynamic loads and higher-order eigenmodes are usually ignored. A numerical analysis [6] indicates that the response specific method underestimates the maximum tower-base moment by over 70% compared to the results of time-domain simulation for a parked wind turbine. Some experimental studies [7-10] also indicate that earthquakes enhance the lateral tower-top displacement significantly to a level that makes it almost impossible to observe meaningful results when using RSM. In comparison, time-varying seismic assessments using the finite element method (FEM) is considered as an alternative method. However, for a proper seismic behaviour assessment of wind turbines, time-domain analysis is required. Traditionally, wind turbines are treated as simplified models that lump rotor and nacelle as a point mass at tower-top [11-15]. The resulting aerodynamic loads are generally neglected or simplified as rotor thrust forces. Based on this simplification, a multi-body dynamic method is employed for an efficient assessment of the responses of wind turbines subjected to earthquake

loadings [16-19]. As prescribed in existing certification guidelines, seismic loading demand is treated as a linear combination of earthquake and wind loads that are calculated individually [20-22]. However, the influence of aerodynamic loads on the dynamic responses of wind turbines cannot be neglected, especially for wind turbines with large diameter rotors [23-24]. The combined effect of aerodynamic and seismic loadings should be included in the time domain analysis of wind turbines subjected to an earthquake event.

In performing the analysis of dynamic responses of wind turbines subjected to wind loads and further excited by ground motion corresponding to the earthquake, a seismic module was added in GH Bladed [6]. With the use of GH Bladed, Santangelo *et al.* [25-26] conducted a set of time-domain simulations for the wind turbine under multiple loadings. The differences between the results of fully-coupled and uncoupled time-domain simulations were investigated. Katsanos *et al*. [27] also implemented the capability of seismic analysis in HAWC2. The dynamic response of an OWT under wind and wave loadings coupled with earthquake excitation has been obtained using HAWC2. On the basis of the results of the three typical operating scenarios (operational, parked and emergency shutdown), a fragility analysis was performed. Meanwhile, Asareh and Prowell developed a numerical analysis tool named Seismic, for the conduct of seismic analysis of wind turbines using FAST [28-30]. In this Seismic tool, a damped actuator was located at the base of the tower in order to replace the degree of freedom (DOF) in translational direction. The earthquakes load in each considered direction is calculated using the modal properties of the actuator. Jin *et al*. [31] used the Seismic tool to predict the wind turbine's dynamic responses under combined wind and earthquake conditions. Asareh *et al*. [32] employed the Seismic tool in performing dynamic analysis of a 5MW wind turbine under a set of conditions associated with winds and earthquakes. The relationship between pseudo spectral acceleration (PSA) and demands of tower displacement and tower moment

was discussed. However, it is noted that these literatures focused more on the effect of earthquake on land-based wind turbines. With the growing global interest in offshore wind power, it is necessary to investigate the seismic behaviour of OWTs. It is important to note that any investigation on this topic should include the interactions between aerodynamic, hydrodynamic and seismic responses due to the increased nonlinearities from the hydrodynamic loading. In addition, the soil effect, which has a significant influence in the dynamic responses of OWTs under earthquake excitations compared to the land-based wind turbines due to their larger dimension, should be included in any study.

Kim *et al.* [33] investigated the seismic fragility of a monopile OWT. Using the ***p-y*** curve method, the soil-structure interaction (SSI) was modelled as a set of springs. Based on the responses of the wind turbine for 22 different earthquakes, it was found that the prediction of fragility is significantly influenced by the variation of earthquake ground motion through different soil layers. Mo *et al.* [34] performed a seismic fragility analysis of an OWT under different operational states by considering the SSI. The probability of reaching damage states was obtained for different wind speed conditions. Alati *et al*. [35] studied the seismic responses of bottom-fixed OWTs under different earthquakes and the soil effect was considered. They found that the resultant demands of tower-base moment and tower-top displacement were significantly increased by the earthquakes. In the emergency shutdown state induced by the earthquake, the blade root bending moment was enhanced, which could not have been be observed in analyses without considering the combined effect of wind and earthquake. For an OWT subjected to an earthquake, the substructure bears the underlying seismic loads and the higher modes of the wind turbine are more likely to be excited. The SSI effects generally play an important role on the seismic loading for OWTs. Despite this, most available literatures model the soil effects on OWT foundation as linear whereas, in reality, this should be modelled as nonlinear. This deficiency therefore constitutes an OWT foundation design problem that should be addressed.

In view of the need to solve such a fundamental problem, this study examines the influence of combined loadings on the OWT foundations. This is achieved following the development and integration of a module, QuakeDyn, into FAST to form the novel seismic analysis framework (SAF). The simulation of the coupled OWT foundation models with nonlinear SSI has been noted as major shortcomings of the existing numerical tools [28-30]. Therefore, this tool (SAF) makes it possible for the dynamic behaviour of an OWT with flexible or fixed foundations subjected to seismic loadings to be adequately simulated by including the SSI. The earthquake loads are evaluated using a more generic method that is commonly used in the seismic analysis of buildings. The SSI model is represented by a set of nonlinear lateral springs whose stiffness is determined using LPILE in order to better reflect the actual response of wind turbines. By using SAF for the analysis, seismic behaviours of the wind turbine under three typical operating states, *i.e*. operational, parked and emergency shutdown conditions triggered by the earthquake are obtained. The differences between the results corresponding to the fixed and flexible foundations are presented in the time domain and frequency domain for a better understanding of the SSI effect. Furthermore, the maximum responses of the wind turbine with both flexible and fixed foundations under different wind conditions are obtained to illustrate the significance of wind loading in seismic analysis. In addition, the direction of ground motions with respect to the inflow wind direction has been considered in examining the intersectional effect of wind and earthquake loadings.

This paper is organized in five sections. The environment loadings are presented in Section 2. Section 3 describes the development of SAF. The results obtained from the investigations are presented and discussed in Section 4, while the findings and conclusions are presented in Section 5.

2 Descriptions of the models and load cases

2.1 Reference wind turbine model

In order to support concept studies of onshore and offshore wind technology, the National Renewable Energy Laboratory (NREL) developed a 5 MW wind turbine known as "NREL 5MW wind turbine" [37]. The NREL 5MW wind turbine with monopile was used in the Offshore Code Comparison Collaboration (OC3) project to demonstrate the suitability of monopile for applications in 20 m water depth areas [38]. The OC3 project used a monopile which has a length of 30 m above the mudline and a penetration of 36 m. The diameter along the monopile (D) is 6 m. This study employs the NREL 5MW monopile OWT as the examined model whose geometry and main specifications are presented in Fig. 2.

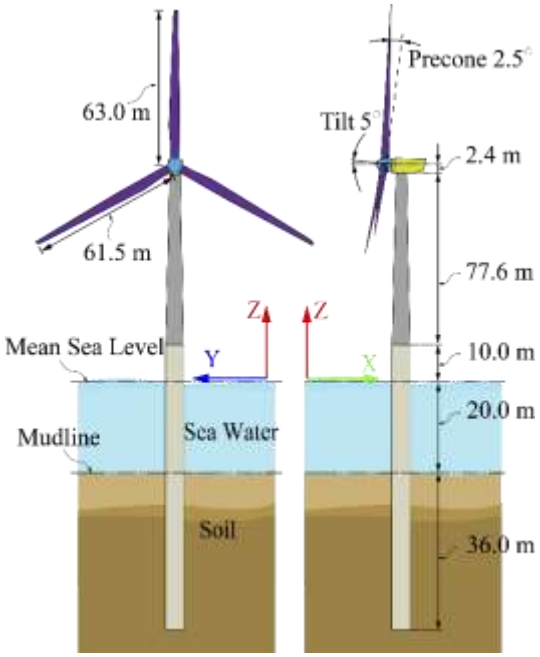

Fig. 2: Schematic diagram of the NREL 5 MW monopile OWT

2.2 Soil-pile interaction model

In modelling the soil structure interaction of the NREL 5MW monopile OWT, a layered soil profile is considered with relatively softer soil in the upper layer and denser soil in the lower layer. The SSI between monopile and the soil has been modelled using coupled springs placed at the

mudline as reported in several recent studies [34-35, 39-42]. A notable shortcoming of this method is that the responses of the embedded pile cannot be obtained correctly. As an alternative means of overcoming the shortcomings, the Winkler spring-dashpot model is well suited for modelling pile in a multi-layered soil condition to reveal the soil-pile interaction more specifically. Fig. 3 presents a schematic diagram of the soil condition and the Winkler model adopted in this study. The springs are distributed linearly from the mudline to the pile bottom at spacing of 1m apart. For each depth, 2 orthogonal springs are used to represent the lateral soil reactions as recommended by the OC3 project.

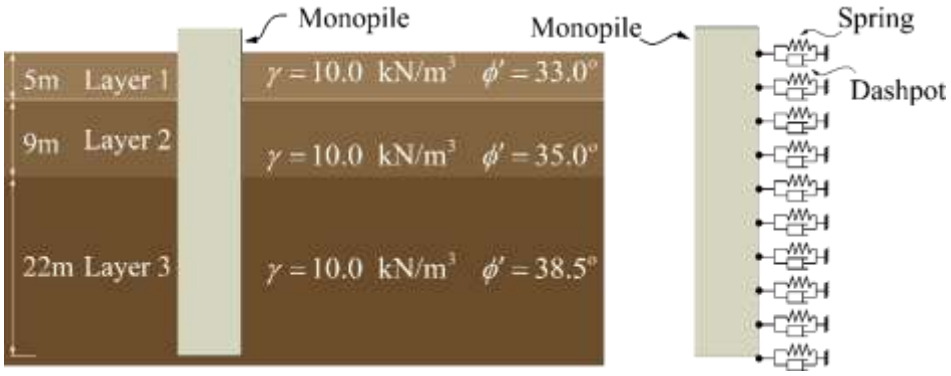

Fig. 3: The soil condition and Winkler model adopted in this study

Each of the soil layers is defined as a sandy soil but with different properties in accordance with the design parameters in the OC3 project. This study used the nonlinear *p-y* curves of the Winkler springs under cyclic loadings obtained using LPILE by Passon *et al.* [43]. Each of the soil layers is defined as a sand based on the American Petroleum Institute (API) recommendation. A shear force of 3.91 MN, a bending moment of 124.4 MN·m and an axial load of 8.6MN are applied at the pile head to define the cyclic loading. The number of cycles of the loading is 5000. With the use of LPILE, the nonlinear *p-y* curves corresponding to the springs at different depths are obtained and presented in Fig. 4. It should be noted that API criteria are used in LPILE for the determination of *p-y* curves. The API method is pertinent and efficient in calculating *p-y* curves for piles with diameter less than 2 m. *Yang et al.* [44] investigated the discrepancy of soil reaction between the API model and finite element

(FE) model in ABAQUS for piles with different diameters. It was found that the difference between the maximum bending moments from the API and FE results is 6.5% for the 6 m diameter pile. In another study, API *p-y* curves were used by Kim *et al.* [33] for a fragility analysis of an offshore wind turbine under earthquake excitation uncoupled with wind loading. Sahasakkul *et al.* [45] conducted a comparative study on the *p-y* curves between the API and FE models for a 5MW OWT. The differences in responses of fore-aft tower-top displacement and out-of-plane bending moment at tower-base were around 5% and 3% for the examined condition respectively. Although the API method is not absolutely perfect in determining the nonlinear *p-y* curves for a large diameter pile, nevertheless it has been extensively used for offshore monopile design [46-49] and it has also been recommended in several design guidelines [50-52]. Furthermore, the *p-y* curves used in this study have also been used in OC3 project (for a 6m diameter pile), a well-known project, for the validation of concepts and numerical tools for OWT design.

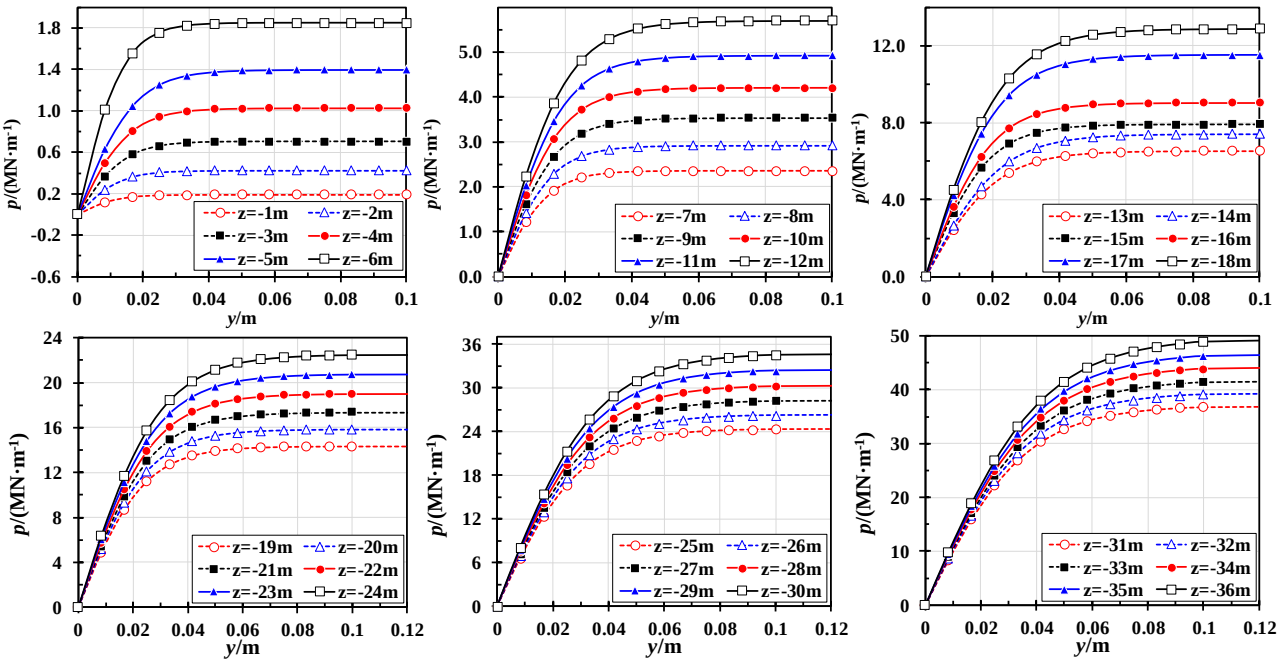

Fig. 4: *p-y* curves of the springs derived using LPILE (z denotes the depth below the sea bed) [43]

The radiation damping due to diffracted waves spreading away from the pile and the material

damping due to hysteretic action in the soil are considered. The model developed by Gazetas *et al.* [53] is used for the damping calculation.

$$C = 6\rho_s V_s d(\frac{\omega d}{V_s})^{-1/4} + 2\beta_s \frac{k_s}{\omega} \quad (1)$$

where C is the damping; ρ_s and V_s are the mass density and shear wave velocity of the soil, respectively. D is the diameter of the pile. ω is the first natural angular frequency of the support structure. β_s is the hysteresis damping ratio with a value of 5% as suggested by Gazetas *et al.* [53]. k_s is the stiffness per unit length of the pile that could be derived by *p-y* curves.

The soil reaction F_s due to relative displacement d_s and velocity v_s between the support structure and soil is derived as:

$$F_s = -k_s \cdot d_s - C \cdot v_s \quad (2)$$

Table 1 presents the natural frequencies of the wind turbine with the fixed and flexible foundations. As shown in Table 1, the eigen-frequencies for the support structure of the flexible foundation model are lower than those of the fixed foundation model as expected. It is noted that the natural frequencies of the 2nd flap modes of the blade changed with the soil effect.

Table 1: The natural frequencies of the wind turbine with flexible and fixed foundations

Mode	Description	Flexible	Fixed
1	1st order Fore-Aft mode of the support structure	0.249	0.277
2	1st order Side-Side mode of the support structure	0.248	0.274
3	1st order drivetrain torsion mode	0.600	0.607
4	1st order asymmetric flapwise yaw mode of the blade	0.660	0.660
5	1st order asymmetric flapwise pitch mode of the blade	0.666	0.665
6	1st order collective flap mode of the blade	0.694	0.696

7	1st order asymmetric edgeise pitch mode of the blade	1.077	1.078
8	1st order asymmetric edgewise yaw mode of the blade	1.088	1.089
9	2nd order Fore-Aft mode of the support structure	1.534	1.867
10	2nd order Side-Side mode of the support structure	1.383	1.589
11	2nd order asymmetric flapwise yaw mode of the blade	1.938	1.833
12	2nd order asymmetric flapwise pitch mode of the blade	2.016	1.932
13	2nd order collective flap mode of the blade	2.106	2.020

In Fig. 5 the normalized modal shapes of the support structure above the mudline are presented. A significant difference between the flexible and fixed foundation models was observed in each mode, especially the 2nd order mode. This implies that the flexibility of foundation plays an unneglectable role in the vibration behaviour of the support structure.

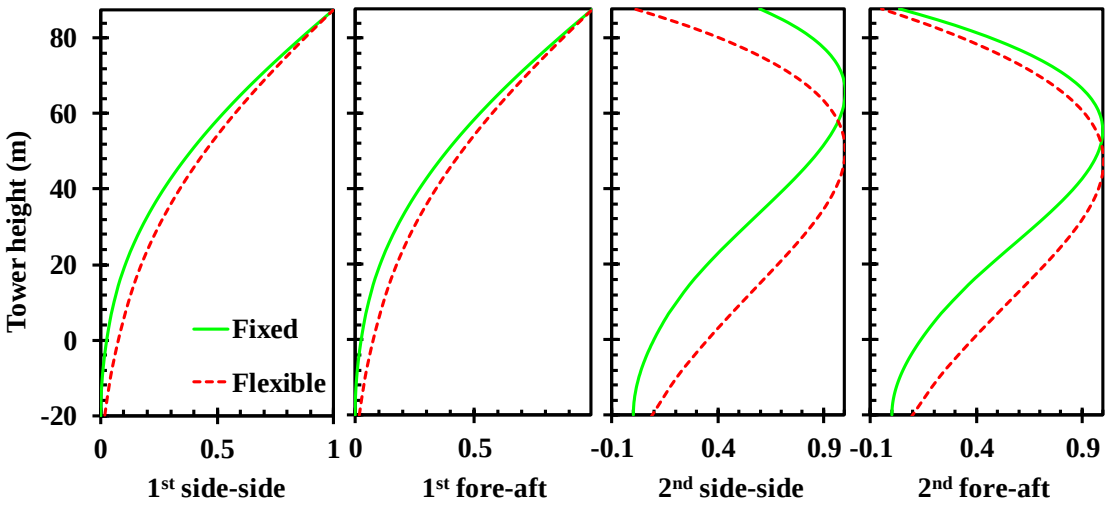

Fig. 5: Normalized modal shapes of the support structure above the mudline

3 Development of Seismic Analysis Framework (SAF)

In order to accurately model the combined effects of earthquake, irregular wave and turbulent

wind on the OWT, a newly developed QuakeDyn module is integrated into an open source code numerical tool, FAST. This tool makes it possible for accurate simulations of OWT subjected to earthquake loadings, SSI and environment conditions (wind, wave and current) to be made using FAST for the first time.

3.1 Description of FAST

FAST is an aero-hydro-servo-elastic simulation tool developed by NREL for both land-based and offshore wind turbines [54]. The original version of FAST consists of different modules (AeroDyn, HydroDyn, ServoDyn and ElastDyn) for performing structural dynamic simulation in time domain. The blades aerodynamic loads are calculated using the Blade Element Momentum Theory (BEMT) approach in the AeroDyn module based on the axial and tangential induction factors which are evaluated by the general Dynamic Wake Model (DWM) and corrected with the Prandtl tip-loss and hub-loss models. The Beddoes-Leishman stall model is applied to estimate the dynamic response of airfoils.

Hydrodynamic loads on the support structures are calculated in the HydroDyn module. The hydrostatic stiffness contributions are included in the hydrodynamic calculation. The drag effect is evaluated using Morison's equation. The added mass and damping contributions from wave scattering in regular or irregular sea are considered in the module.

In the ElastDyn module, the structural dynamics are calculated based on a multi-body dynamics method and a linear modal approach with prescribed mode shapes of the flexible bodies. The first two flapwise eigenmodes and the first edgewise eigenmode of the blades are included. The first two fore-aft and side-side eigenmodes of tower are also considered.

The blade pitch and rotational speeds of the rotor and generator can be controlled in ServoDyn

through dynamic link libraries and an interface with Simulink or Labview. The Fourth-order iterative methods (Adams-Beshforth, Adams-Mounton and Runge-Kutta) are used for the execution of the time marching simulation.

3.2 Seismic analysis framework

The SAF is developed as a user-developed tool following the integration of the newly developed QuakeDyn module into FAST in order to provide the coupled nonlinear SSI - seismic analysis capability. The earthquake force acting on the wind turbine is calculated based on the support structure's normalized mode shapes and the input accelerograms. A schematic diagram of SAF showing the integration of the QuakeDyn module in FAST is presented in Fig.6. The SAF makes it possible for the soil effects on OWT foundation during an earthquake to be accurately modelled using nonlinear lateral springs.

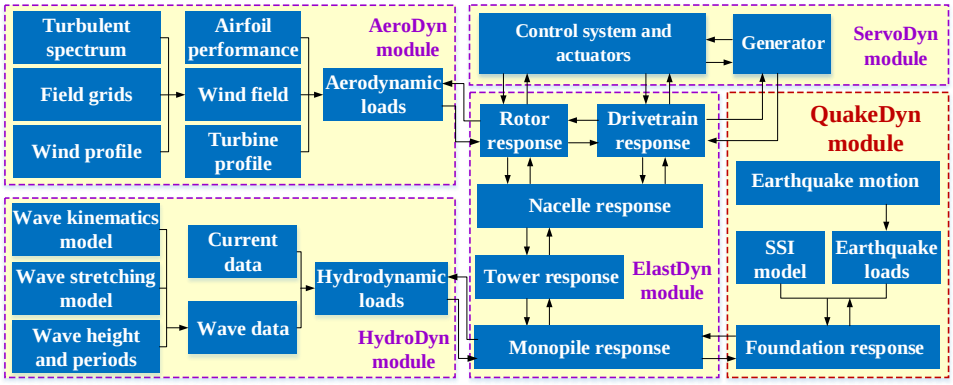

Fig. 6: Schematic diagram of SAF

In the QuakeDyn module, the calculation of the earthquake loads acting on the support structure is based on the generic method that is widely used in the seismic analysis of buildings. The earthquake force associated with each mode of the support structure, $F_{\mathrm{eq},i}$, is derived as:

$$F_{\mathrm{eq},i} = a_{\mathrm{eq,hor}} \cdot \int_0^H [m(h) \cdot \phi_i(h)]\mathrm{d}h \qquad i = 1,2,3,4 \tag{3}$$

where $a_{\mathrm{eq,hor}}$ is the horizontal acceleration of input ground motion. $m(h)$ and $\phi_i(h)$ are the mass density and the *i*th normalized mode shape of the support structure, respectively. *H* is the length of the support structure.

The nacelle and rotor are treated as a given mass atop the support structure. The earthquake force acting on the tower-top components, $F_{\mathrm{eq,top}}$, is derived as:

$$F_{\mathrm{eq,top}} = a_{\mathrm{eq,hor}} \cdot m_{\mathrm{top}} \tag{4}$$

where m_{top} is the sum of the rotor and nacelle masses.

The vertical earthquake force of the whole wind turbine, $F_{\mathrm{eq,ver}}$, is applied at the base of the support structure and calculated as follows:

$$F_{\mathrm{eq,ver}} = a_{\mathrm{eq,ver}} \cdot m_{\mathrm{turbine}} \tag{5}$$

where $a_{\mathrm{eq,ver}}$ is the vertical acceleration of the input ground motion and m_{turbine} is the mass of the whole wind turbine.

The earthquake loads are added into the active force component of the equation of motion established in FAST [54]. Therefore, the earthquake loads are combined with other environmental loads, including aerodynamic loads, hydrodynamic loads and gravitational force, in order to perform nonlinear SSI-coupled dynamic simulations.

3.3 Validation of SAF

In order to validate the reliability of the SAF, a benchmark study using a commercial software package, GH Bladed and a seismic analysis tool developed by NREL (called “NREL Seismic”) [28] is conducted. Although NREL Seismic is not specifically designed to examine the flexible foundation and nonlinear soil effects for wind turbines subjected to earthquakes, the tool is capable of performing the seismic analysis of fixed foundation wind turbines. This validation is therefore carried on a fixed

foundation of an OWT only. In order to avoid any discrepancy in the calculations of aerodynamic load for validation using both FAST and GH Bladed, the wind turbine is assumed to be parked. The structural damping ratio of the support structure for the wind turbine modelled in the three tools is kept the same with a value of 1%. The El Centro earthquake record with two horizontal components is selected as the input ground motion. The earthquake is assumed to occur at the 800^{th} s. Dynamic responses of the NREL 5 MW OWT with a fixed foundation calculated using SAF and the two numerical tools are presented in Fig. 7. It is observed that the predictions from SAF are in line with the ones obtained using GH Bladed and NREL Seismic. Slight difference between SAF and GH Bladed is observed for the tower-top displacement. Regarding the fore-aft tower-top acceleration, the results of SAF agree with that of GH Bladed due to the similarity in their methodology for earthquake load calculation. However, the discrepancy between the results of NREL Seismic and GH Bladed is large. Similar observations were made for the out-of-plane mudline bending moment. As mentioned in the introduction, a major shortcoming of NREL Seismic is the reliance on the experience of engineers in the selection of the values of stiffness and damping for earthquake load calculation. The agreements between the compared results indicate that SAF has a higher fidelity and can be used for the assessment of the seismic behaviour of fixed foundation wind turbines. This confirms that SAF can be extended to the flexible foundation model since the algorithm has been appropriately enhanced.

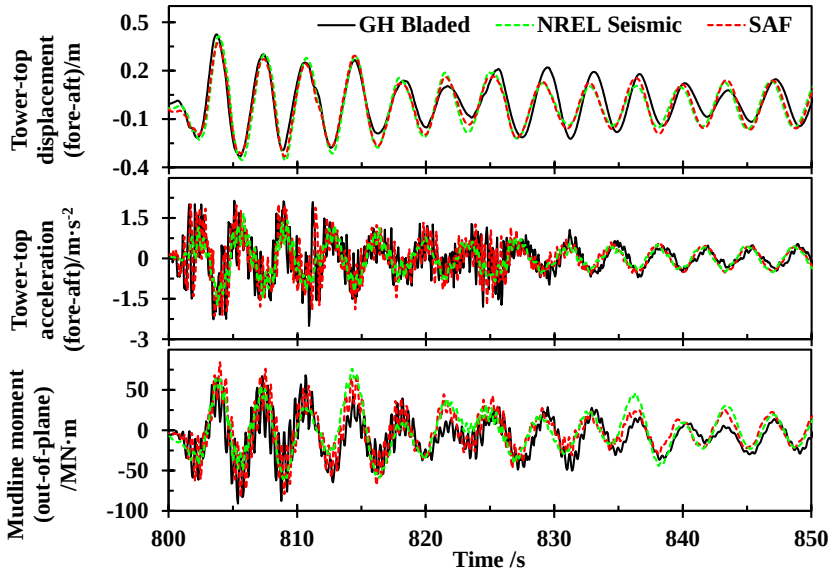

Fig. 7: Comparisons of the results calculated with SAF and reference numerical analysis tools

4 Results and Discussions

4.1 Soil effect under different operating states

This study aims to examine the soil effect on the dynamic behaviour of an OWT subjected to an earthquake coupled with wind loading. The Chi-Chi earthquake with a magnitude of 7.3 is selected as the input ground motion. The accelerograms of the earthquake event recorded by the TCU071 station are used. The earthquake record consists of 2 horizontal and 1 vertical components and the PGA is 0.546 g. Fig. 8 presents the 0.5% damped spectral acceleration of the earthquake record. From this figure, it is noted that the 2nd eigenmode of the support structure may have a noticeable contribution to the structural response due to its short fundamental period which falls within the range of significant spectral accelerations.

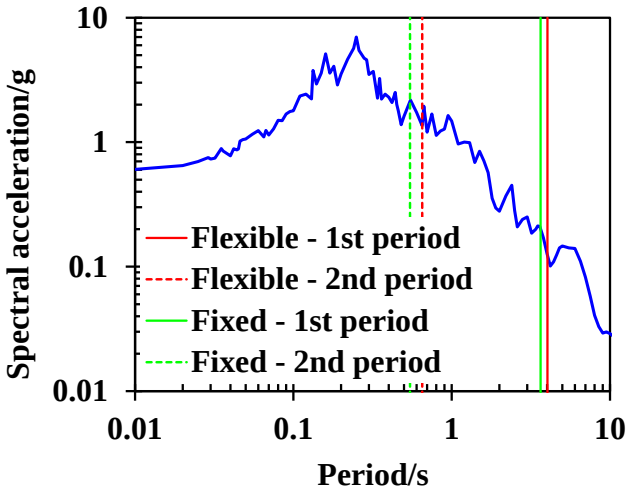

Fig. 8 Spectral acceleration of the Chi-Chi TCU071 earthquake record

The record of the earthquake accelerations is presented in Fig. 9. More details of the earthquake event can be found in the Pacific Earthquake Engineering Research (PEER) database [55]. The ground motion is referred as the motion of the sea bed surface. Based on the input ground motion, the earthquake loads applied to the support structure are calculated and then coupled with aerodynamic and hydrodynamic loads acting on the wind turbine system.

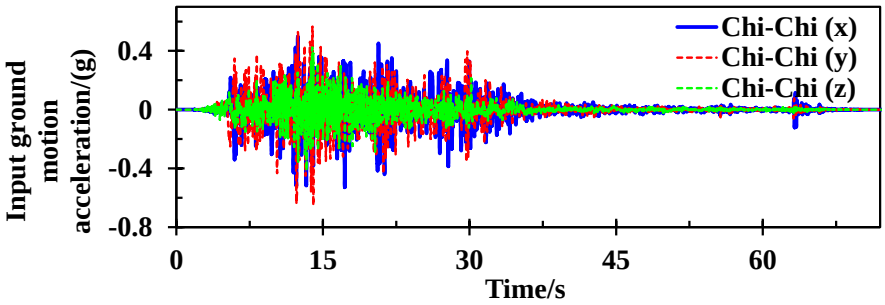

Fig. 9: Acceleration history of the Chi-Chi TCU071 earthquake record

In order to obtain a preliminary insight into the soil effect on the dynamic responses of wind turbine subjected to multiple loadings associated with wind, wave and earthquake, the time domain responses of the wind turbine with fixed and flexible foundations are discussed for the following operating states: (a) operational, (b) parked and (c) emergency shutdown (induced by earthquake). For the operational state, the wind turbine is in operation. TurbSim is used to generate a full-field

turbulent wind with an average velocity of 11.4 m/s based on Kaimal wind spectrum [56]. The wave period and significant wave height are 10.5 s and 6.3 m, respectively [57]. The Airy wave theory is used to generate the wave histories based on JONSWAP wave spectrum [58]. For the emergency shutdown scenario, the wind and wave conditions are the same as that of the operational state. The generator will be disconnected and the blades will be pitched to feather with a pitching rate of 8 deg/s once the square root of the sum of the squares (SRSS) of nacelle acceleration exceeds the threshold value. For the determination of the threshold value, the peaks of the SRSS of nacelle accelerations for the wind turbine under different wind conditions without earthquake excitation are obtained and presented in Fig. 10. The values of SRSS of nacelle accelerations are smaller than 1 m/s^2 for the wind speeds within the design operation range. With a safety factor of 2, the threshold acceleration value is selected as 2 m/s^2 in this study. For the parked state, the mean wind velocity at hub is 30 m/s. This is higher than the wind turbine's cut-out wind speed. The wave period and height used herein are respectively 16.5 s and 12.0 m, respectively [58]. The manner of operation in this condition is such that the generator is disconnected and the blades are fully feathered. For all the considered conditions, the simulation duration is 1000 s and the time step is 0.002 s. The earthquake is assumed to occur at 800^{th} s to ensure that the wind turbine has already been operating in a steady state [28]. Table 2 presents the conditions of each load case for both the fixed and flexible foundation models.

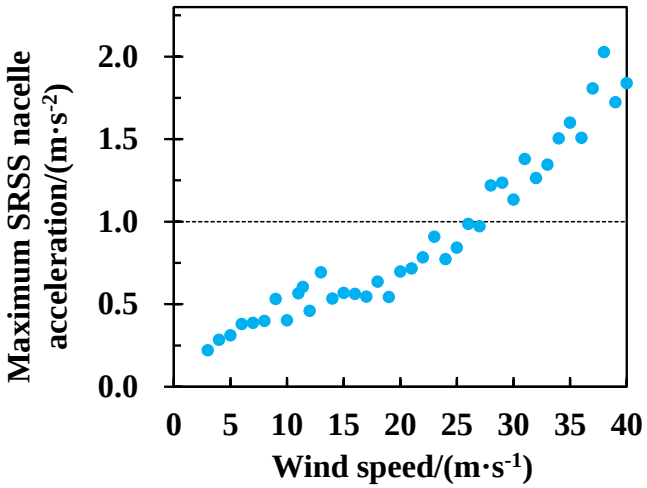

Fig.10: The peaks of the SRSS nacelle acceleration under different wind conditions

Table 2: Simulation cases for the examination of soil effect under different operating states

	Operating State	Wind Speed	Wave period	Wave height	Earthquake
Case 1	Operational	11.4 m/s	10.5 s	6.3 m	Chi-Chi
Case 2	Emergency shutdown	11.4 m/s	10.5 s	6.3 m	Chi-Chi
Case 3	Parked	30.0 m/s	16.5 s	12.0 m	Chi-Chi

In Fig. 11, the tower-top displacements and mudline bending moments of the wind turbine with fixed and flexible foundations in the three aforementioned operating states are presented. Obvious discrepancies of amplitudes and variation between the results of the different foundations are observed, indicating that the soil flexibility has a notable influence on the dynamic characteristics of wind turbine subjected to an earthquake event.

In the operational state, the mudline bending moments and tower-top displacements increase significantly with the values fluctuating once the earthquake occurs (> 800 s), and reduce progressively after the strong shaking (> 820 s). The amplitudes of the fixed foundation case decrease

more rapidly than those of the flexible foundation with regards to the out-of-plane mudline bending moment and the tower-top's Side-Side displacement. The resultant mudline moment and tower-top displacement of fixed foundation are significantly smaller than those of the flexible case after the earthquake stroke (>800 s). The difference in the results between the two cases is insignificant before the occurrence of the earthquake. It can be argued that a larger modal shape magnitude of the flexible model results in a relatively larger earthquake force, implying that the dynamic responses are underestimated if the soil effect is ignored.

It is reasonable to assume that the tower displacement consists of vibration amplitude and elastic deformation. Due to the absence of aerodynamic loads in the side-side direction, the amplitude of vibration induced by the earthquake dominates the side-side displacement. If the earthquake occurs, a more severe side-side vibration of the support structure would be caused in the flexible base condition. As shown in Fig 11-(a), in both fore-aft and the side-side directions, the flexible foundation model has larger displacements than those of the fixed foundation. The fore-aft displacement of the two models are approximate 0.5 m before the earthquake, while the maximum fore-aft displacements of the flexible and fixed cases are over 1.5 m. It implies that the severe vibration induced by the earthquake dominates the tower-top displacements.

In the parked state, since the blades are fully feathered, the aerodynamic load acting on the rotor is insignificant compared with the wave and earthquake loads. It means that the elastic deformation induced by the aerodynamic load is much smaller than the vibrational amplitude caused by the earthquake loads. As can be seen from Fig. 11 (b), the average values of tower-top fore-aft displacement in the fixed and flexible cases are very close. In the parked state, the peaks of the tower-top fore-aft displacement in the fixed and flexible conditions are 1.77 m and 2.25 m, respectively while the values in the operational state are 1.63 m and 2.10 m. This indicates that the aerodynamic

damping has a positive effect in mitigating the vibration amplitude because of energy dissipation resulting from aerodynamic damping during earthquake event. This finding is consistent with the conclusion for a land based wind turbine under earthquake events [59].

In the case of emergency shutdown condition induced by the earthquake, the generator is turned off at 808.468 s and 807.336 s for the fixed and flexible cases, respectively. The variations of the results in the emergency shutdown state are significantly different from those in the operational state, especially for the fore-aft responses. As a result of emergency shutdown, for both the fixed and flexible cases, the tower-top fore-aft displacement deviates rapidly from a positive value to a negative one. When the blades are fully feathered (time history above 818 s), the variation of the tower-top's fore-aft displacement is similar to the results of the parked state. Nevertheless, the peak amplitudes of flexible cases are significantly greater than those in the parked and operational states. It can be concluded that the emergency shutdown has no expected beneficial effects in mitigating the adverse dynamic responses of the wind turbine subjected to earthquake events.

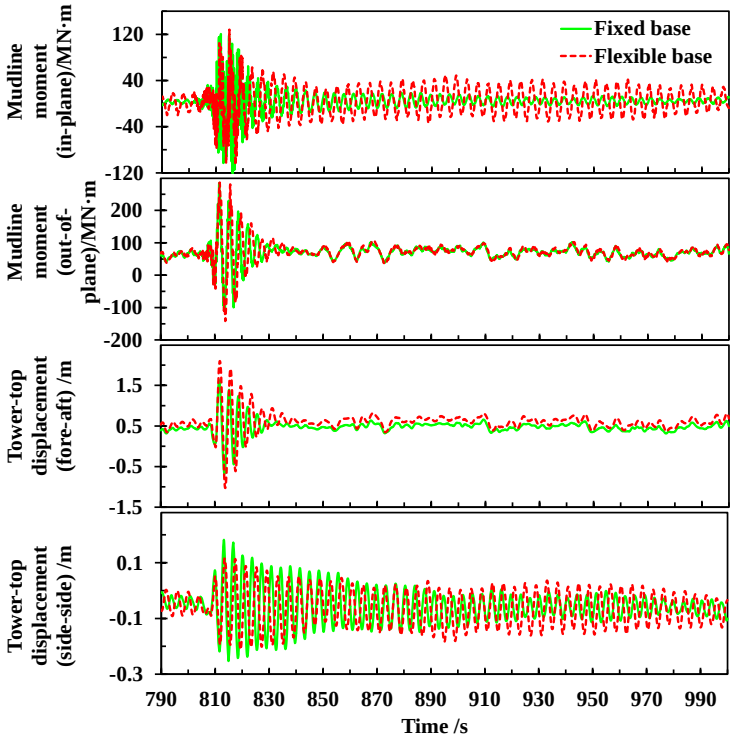

(a) Operational

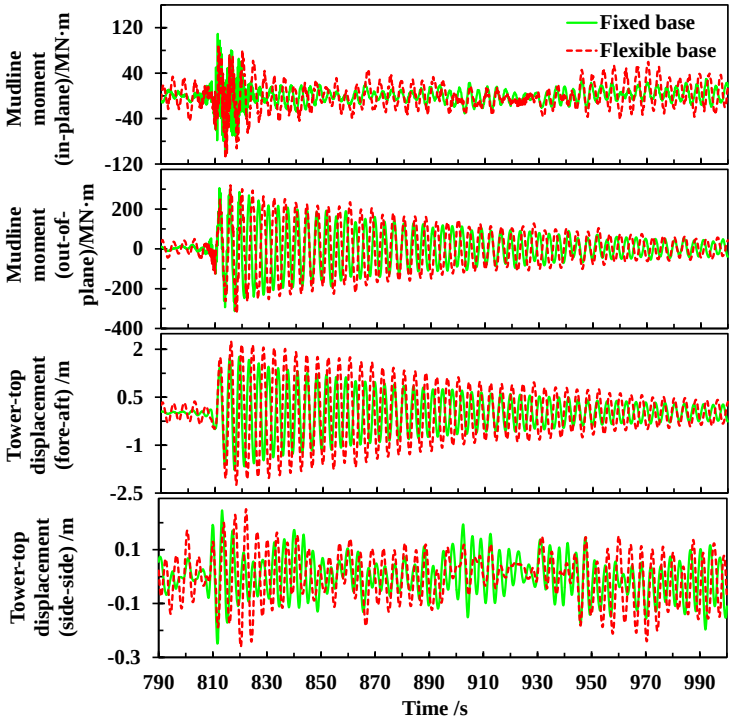

(b) Parked

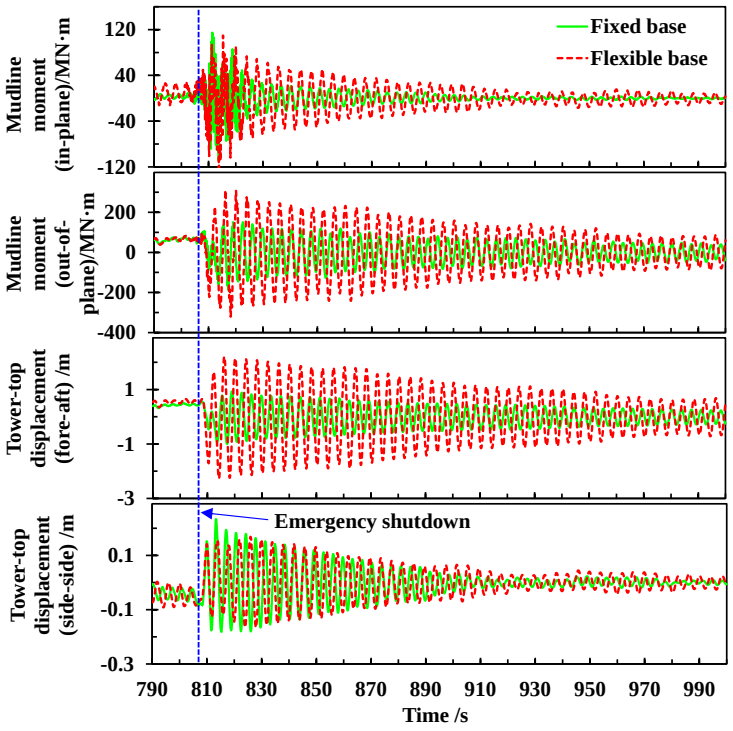

(c) Emergency shutdown induced by earthquake

Fig. 11: Responses of the monopile wind turbine with different foundation conditions for the examined operating states

In order to reveal the vibration characteristic of the support structure under the earthquake excitation, the frequency domain results are obtained by applying Fast Fourier Transformation (FFT) on the tower-top displacements histories, as presented in Fig. 12. In the operational state, the activations of the 1st fore-aft mode of the support structure for the fixed and flexible foundation models are confirmed by the fact that the obvious peaks are observed. As expected, the peak values are found at around 0.25 Hz and 0.28 Hz for the flexible and fixed cases, respectively. Furthermore, the peak amplitude of the flexible case is slightly larger than that of the fixed case. Similar observations were made in the parked and emergency shutdown states. It is noted that the amplitude at 0 Hz is one order lower than that at the 1st natural frequency for the parked and emergency shutdown scenarios due to the absence of aerodynamic effect. Once again, this implies that the aerodynamic loads have a beneficial effect of eliminating the vibration induced by the earthquake.

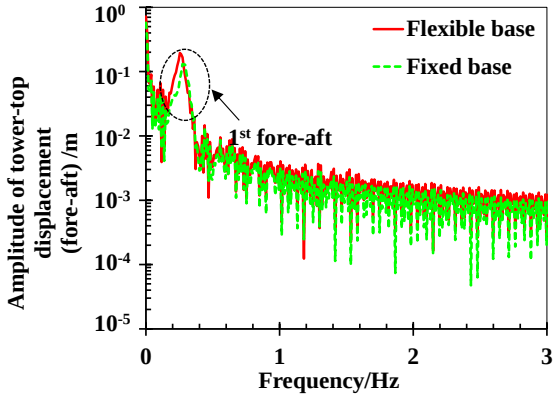

(a) Fore-aft displacement of the operational state

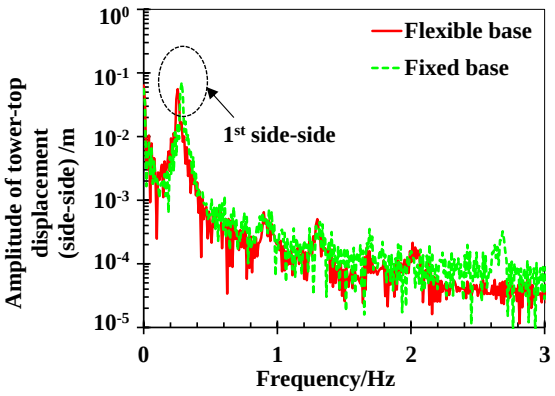

(b) Side-side displacement of the operational state

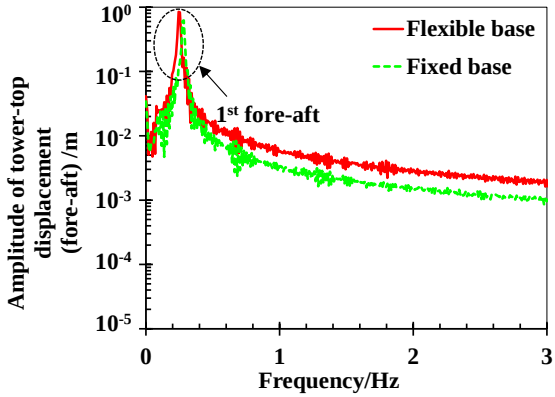

(c) Fore-aft displacement of the parked state

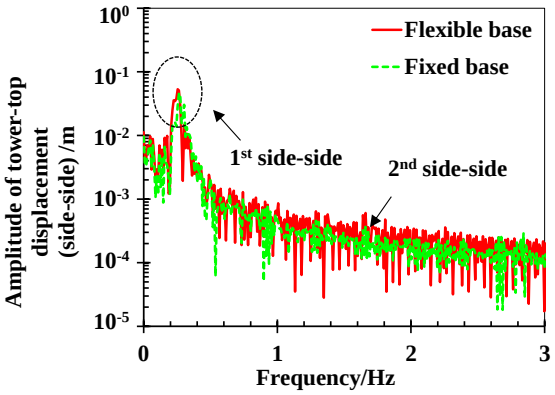

(d) Side-side displacement of the parked state

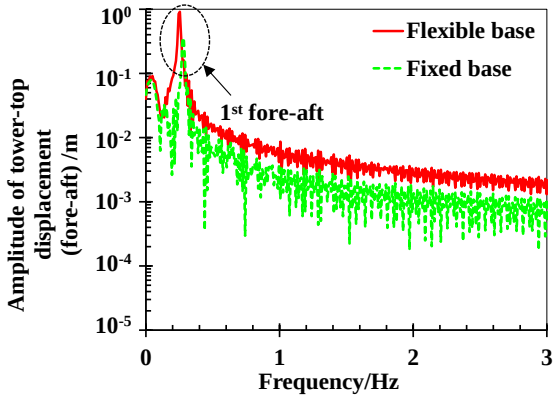

(e) Fore-aft displacement of the emergency shutdown state

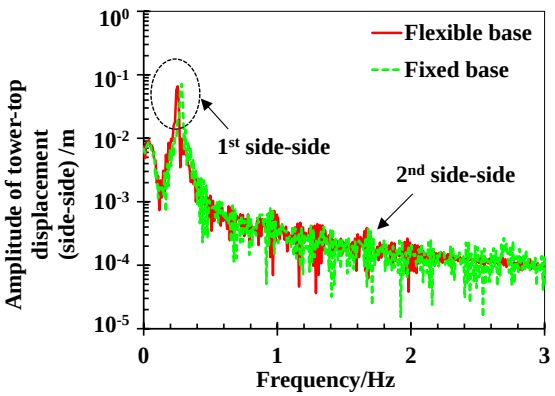

(f) Side-side displacement of the emergency shutdown state

Fig.12: The frequency domain results of the tower-top displacements

Regarding the results in the side-side direction, the 2nd mode is activated for the flexible case in parked and emergency shutdown operation conditions. This observation is invisible in the fixed base model. In addition, the amplitude at the 1st eigen-frequency of the flexible case is much larger than that of the fixed case, indicating the flexible foundation is more sensitive to the earthquake loads.

In Fig. 13, the maximum displacements and bending moments along the support structure above the mudline are presented. In the operational states, the difference between the moment demands of the fixed and flexible cases are insignificant, implying that the fixed foundation model can be properly used for seismic loading demands analysis of OWT. Nonetheless, it is noted that large discrepancies of displacement between the fixed and flexible cases are observed for all examined operating states. As can be seen in Fig. 13 (a) and Fig. 13 (b), the moments at the base and the displacements at the top in the operational state are smaller than those in the parked state for both foundation types. As stated previously, due to energy dissipation from aerodynamic damping during earthquake, the turbulent wind offers a positive effect in mitigating the fore-aft vibration amplitude effect. Similarly, as shown in Fig. 13 (a) and Fig. 13 (c), the mudline moment has been decreased by 34.4% due to the shutdown for the fixed foundation, but increased by 8.6% for the flexible foundation. The reason for the observations is that the transient instability of vibration attributed to the abrupt change of aerodynamic loads induced by the emergency stop cannot be eliminated efficiently from a flexible foundation. It indicates that ignoring the soil effect may cause a misjudgement regarding the results of the emergency shutdown state.

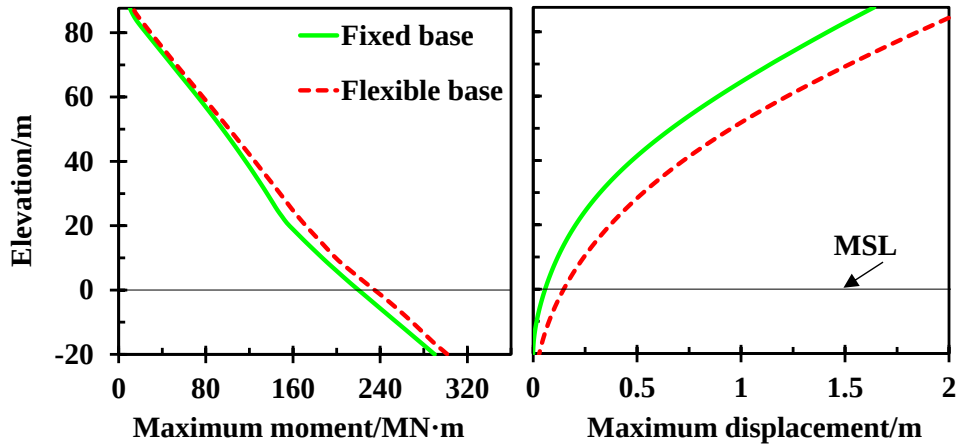

(a) Operational

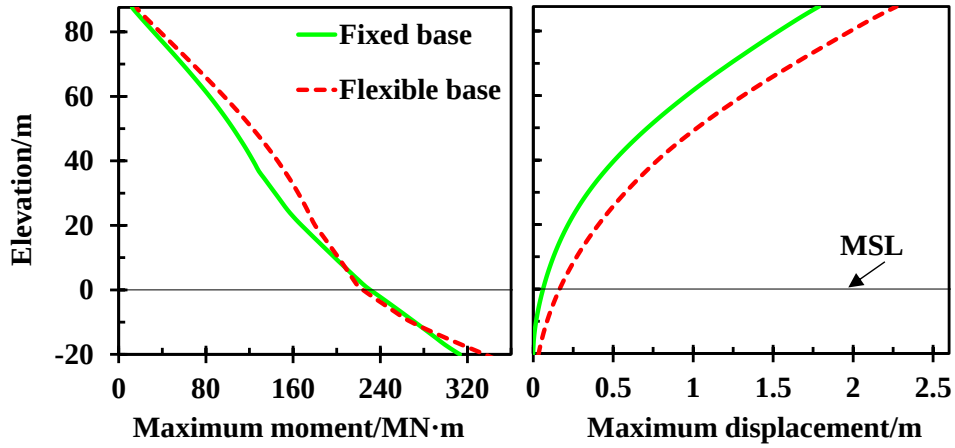

(b) Parked

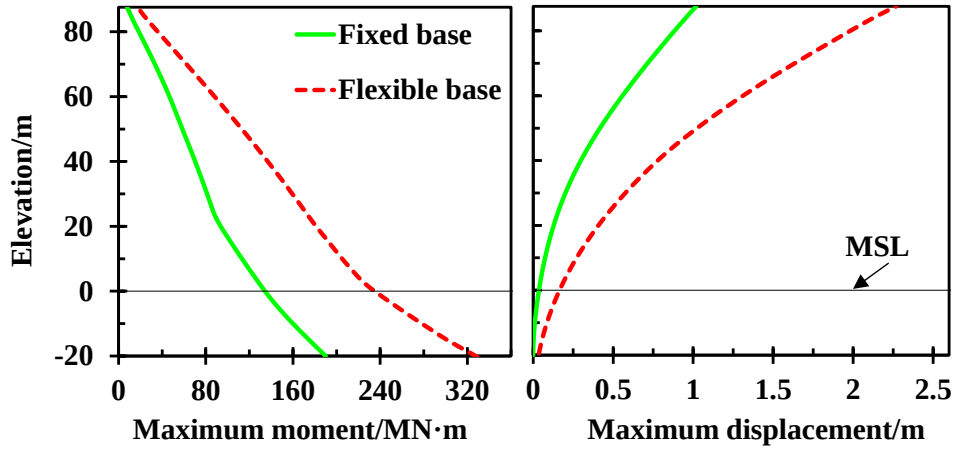

(c) Emergency shutdown induced by the earthquake

Fig. 13: The peaks of displacement and bending moments along the support structure for the examined operating states

The dynamic responses of the wind turbines with fixed and flexible foundations under different wind conditions are obtained in order to confirm the effect of emergency shutdown. In total, 22 wind conditions with different wind speeds are examined. The wave period and height corresponding to each of the wind condition are presented in Table 3. For the both flexible and fixed foundations, operational and emergency shutdown states are examined under each of the load cases presented in Table 3. The criterion for inducing an emergency shutdown is that the nacelle acceleration exceeds a threshold value of $2m/s^2$. Table 4 presents the specific configurations of the examined cases. The Chi-Chi earthquake record presented in Fig. 8 is used as the input ground motion.

Table 3: The wave period and height corresponding to each of the wind speeds

Wind speed (m/s)	Wave height (m)	Wave period (s)
4	1.15	6.47
5	1.80	7.00
6	2.50	7.50
7	2.80	7.70
8	3.11	7.97
9	4.30	8.60
10	5.70	9.30
11	6.05	10.39
12	6.60	10.89
13	7.00	11.00
14	7.34	11.64
15	7.70	12.00
16	8.00	12.23
17	8.30	12.54
18	8.70	13.00
19	9.00	13.37
20	9.40	13.69
21	10.06	14.13
22	10.31	14.46
23	10.70	14.90
24	10.80	15.00
25	11.00	15.20

Table 4: Simulation cases for illustrating the emergency shutdown effect

	Foundation	Wind Speed	Wave period	Wave height	Operating state
Case 1	Flexible	4 ~ 25 (m/s)	6.47 ~ 15.20 (s)	1.15 ~ 11.00 (m)	Operational
Case 2	Flexible	4 ~ 25 (m/s)	6.47 ~ 15.20 (s)	1.15 ~ 11.00 (m)	Emergency shutdown
Case 3	Fixed	4 ~ 25 (m/s)	6.47 ~ 15.20 (s)	1.15 ~ 11.00 (m)	Operational
Case 4	Fixed	4 ~ 25 (m/s)	6.47 ~ 15.20 (s)	1.15 ~ 11.00 (m)	Emergency shutdown

The maximum tower top displacements of the wind turbine with flexible and fixed foundations

are presented in Fig. 14. As can be seen from Fig. 14-(a), the displacements of the flexible foundation case under emergency shutdown states are larger than those from the operational states for most wind conditions. For the most common operating wind conditions (7m/s ~ 15m/s), the shutdown induced by the earthquake increases the displacement by over 10%. This indicates that emergency shutdown has no expected positive effects on mitigating the tower-top response for the flexible foundation wind turbine under most operating wind conditions. On the contrary, emergency shutdown could reduce tower-top displacement efficiently for the fixed foundation wind turbine. In addition, the maximum mudline bending moments of the two wind turbines under operational and emergency shutdown states are presented in Fig. 15. Similar to the observations from Fig. 14, the emergency shutdown cannot efficiently mitigate the mudline bending moment for fixed and flexible foundations under most wind conditions. However, notable decreases are observed for the fixed foundation when the wind speed falls within 8 m/s ~14 m/s.

Comparisons of the results under operational and emergency shutdown states between flexible and fixed foundations have indicated that misjudgements could occur when evaluating the seismic behaviour of the emergency shutdown state if the soil effect is ignored.

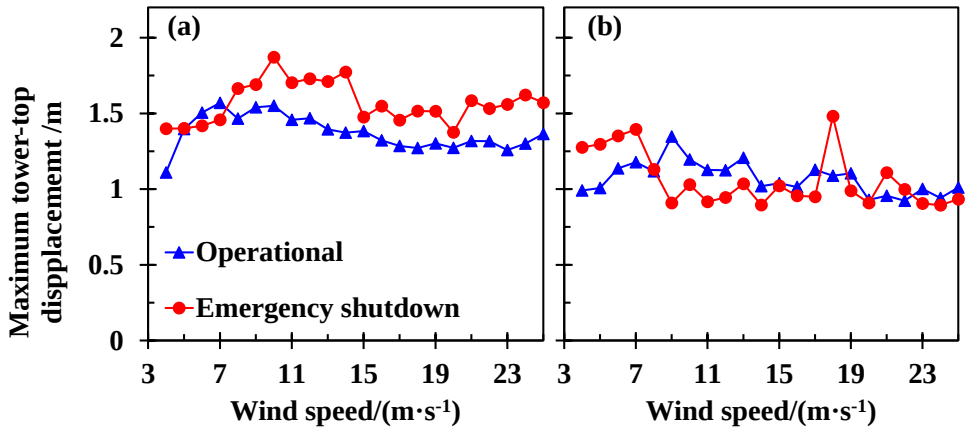

Fig. 14: Maximum tower-top displacement under operational and emergency shutdown states of the wind turbine with (a): flexible foundation, and (b): fixed foundation

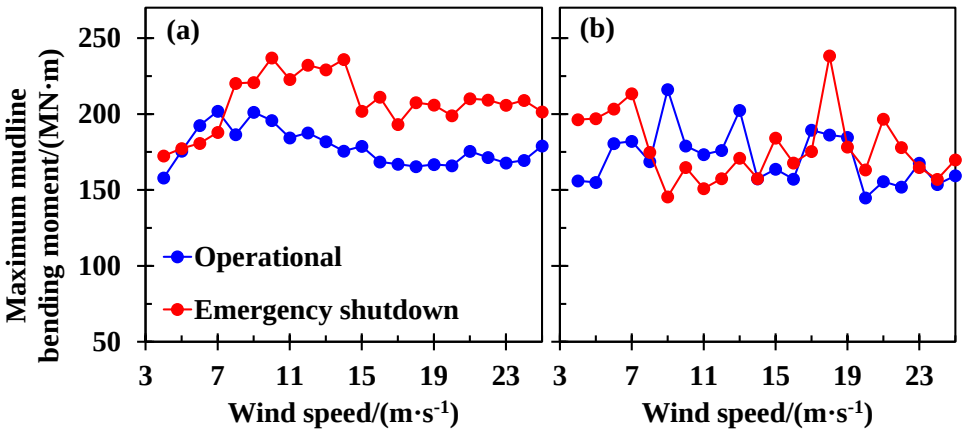

Fig. 15: Maximum mudline bending moments under operational and emergency shutdown states of the wind turbine with (a): flexible foundation, and (b): fixed foundation

4.2 Effect of wind loading

In order to confirm the dominant loading of the wind turbine, the wind only case and wind coupled with an earthquake are examined for both the flexible and fixed foundations. The examination is based on 22 environmental conditions with different wind speeds and wave heights (presented in Table 3). The Chi-Chi earthquake record presented in Fig. 8 is used as the input ground motion for the coupled loading case. Table 5 presents the specifications of the examined cases. In total, 88 simulations have been performed.

Table 5: Simulation cases for the examination of wind loading effect

	Foundation	Wind Speed	Wave period	Wave height	Earthquake
Case 1	Flexible	4 ~ 25 (m/s)	6.47 ~ 15.20 (s)	1.15 ~ 11.00 (m)	Chi-Chi
Case 2	Flexible	4 ~ 25 (m/s)	6.47 ~ 15.20 (s)	1.15 ~ 11.00 (m)	-
Case 3	Fixed	4 ~ 25 (m/s)	6.47 ~ 15.20 (s)	1.15 ~ 11.00 (m)	Chi-Chi
Case 4	Fixed	4 ~ 25 (m/s)	6.47 ~ 15.20 (s)	1.15 ~ 11.00 (m)	-

The maximum tower-top displacements of the wind turbine under different environmental conditions are obtained and presented in Fig. 16. For the wind only cases, the maximum tower-top

displacement of both the flexible and fixed foundation models increases with wind speed reaching the peak at 10m/s condition. Afterwards, it decreases progressively when wind speed is lower than 13m/s. For the conditions with wind speed over 13m/s, the maximum tower displacement slightly fluctuates around the value of the 13m/s case. For the coupled loading case, the maximum tower-top displacements are twice over those from the wind only case for both the flexible and fixed foundation models. Moreover, the trend of the displacement versus the wind speed of the wind only case is invisible for the coupled loading case.

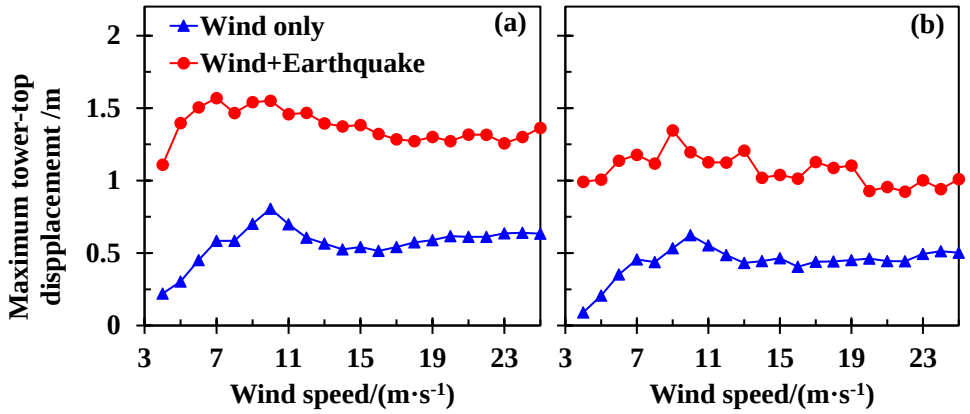

Fig. 16: Maximum tower-top displacement under wind only and coupled loading cases of the wind turbine with (a): flexible foundation, and (b): fixed foundation

Fig. 17 presents the mudline bending moments of the flexible and fixed foundation wind turbines under different wind conditions. The mudline bending moments of the both flexible and fixed foundation models have similar variation trends versus wind speed for the wind only condition. Similar to the observations of displacement, the mudline bending moment reaches the peak at 10m/s wind condition. The magnitudes of the mudline bending moments of the coupled loading case are approximately twice larger compared to those from the wind only condition. The flexible foundation model has larger discrepancies between the two loading cases compared to the fixed foundation model. The comparisons of tower-top displacement and mudline bending moment indicate the earthquake

excitation dominates the dynamic behaviour for all of the wind conditions.

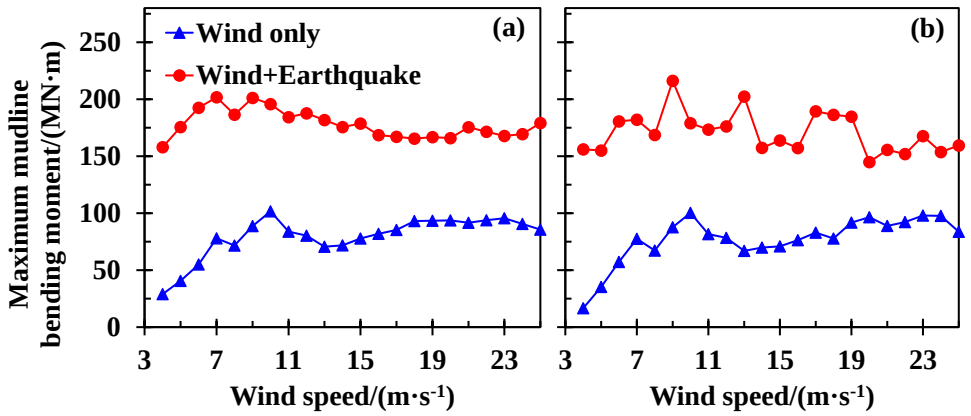

Fig. 17: Maximum mudline bending moment under wind only and coupled loading cases of the wind turbine with (a): flexible foundation, and (b): fixed foundation

4.3 Effect of the ground motion direction

As indicated by the results presented above, wind loading has an unneglectable influence on the dynamic responses of the wind turbine, although the earthquake is the most dominant loading. The direction of the ground motion with respect to the wind direction is considered through changing the intersection angle between the longitudinal component of the earthquake (the x component in Fig. 8) and the inflow wind. The intersection angle varies from 0 degree to 350 degrees by 10 degrees. In total, 72 simulations are performed for the flexible and fixed foundation models. Table 6 presents the specifications of the examined cases.

Table 6: Simulation cases for the examination of interaction effect between wind and ground motion

	Foundation	Wind speed	Wave period	Wave height	Intersection angle
Case 1	Flexible	11.4 m/s	10.5 s	6.3 m	0 ~ 350 degree
Case 2	Fixed	11.4 m/s	10.5 s	6.3 m	0 ~ 350 degree

Fig. 18 presents the maximum and average tower-top displacements and mudline bending

moments under different intersection angles. It has been noted that the intersection effect between ground motion and inflow wind significantly affects the analysis results. For both the flexible and fixed foundation cases, a peak value is observed at the 180-degree scenario or the 0-degree scenario. Similarly, a trough value is observed at the 90-degree or 270-degree scenarios. The flexible foundation case has a peak value of 1.79 m and a trough value of 0.92 m for the tower-top displacement. The peak and trough values of tower-top displacement for the fixed foundation are 1.41 m and 0.69 m, respectively. It is noted that the absolute difference between the peak and trough values for both the flexible and fixed foundations is approximate 50%. A large discrepancy of the mudline bending moment between different intersection angle conditions can be observed as well. The peak and trough values are 236 MN·m and 127 MN·m for the flexible foundation, and the corresponding values are 229 MN·m and 126 MN·m for the fixed foundation. The large discrepancies between different intersectional scenarios indicate that it is necessary to take into account the ground motion direction for seismic analysis of wind turbines. The results presented also indicate that the intersection effect between inflow wind and ground motion can be examined properly by considering only the 0-degree and 90-degree scenarios.

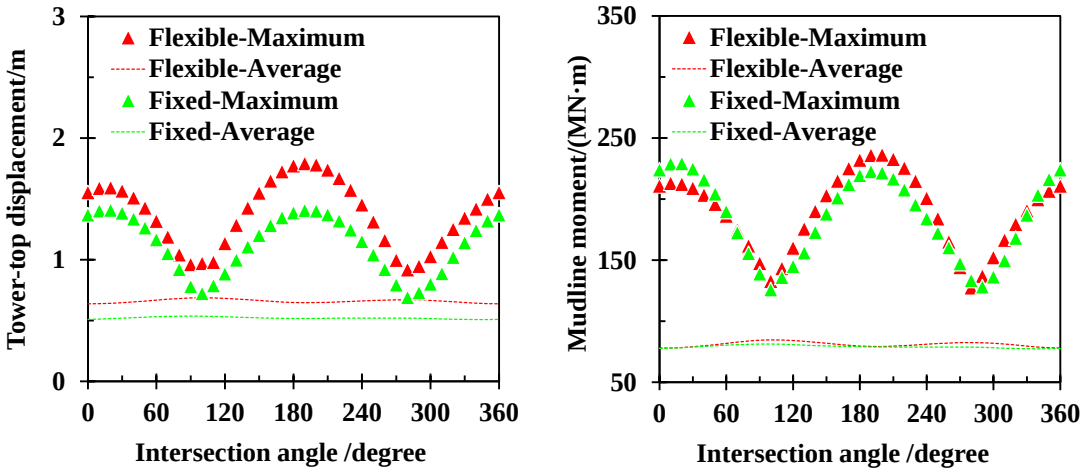

(a) Tower-top displacement (b) Mudline bending moment

Fig. 18: Tower-top displacement and mudline bending moments under different intersection

angle conditions

5 Conclusions

In this study, a multi-purpose SAF consisting of a newly compiled module (QuakeDyn) implemented into the FAST source code is developed and presented. SAF has been validated through comparisons with predictions made using GH Bladed and NREL's numerical analysis tools. The dynamic response of the 5MW NREL monopile OWT with fixed and flexible foundations subjected to wind, wave and earthquake has been investigated using SAF. The flexible foundation is represented by using the nonlinear *p-y* curves obtained using LPILE. Three typical operating conditions, *i.e*. (a) operational, (b) parked and (c) emergency shutdown triggered by earthquake have been considered together with the soil effect. In addition, 22 different wind conditions have been examined to reveal the dominant loading of the wind turbine throughout the design wind speed range. The ground motion direction with respect to the inflow wind direction has been taken into account. Based on the results and discussions presented in the previous section, some key conclusions are presented as follows:

(1) A newly developed module (QuakeDyn) is integrated in FAST in order to establish a generic SAF tool for the investigations of nonlinear SSI and seismic behaviours of OWTs under multiple loading and for different operating conditions. Through comparisons with the results of referenced numerical analysis tools, a good agreement between SAF and the current techniques for fixed foundations has been confirmed. This supports the enhancement of the numerical tool for assessment of the nonlinear SSI effect on flexible foundation, thereby making SAF a valid tool for the assessment of seismic behaviours for wind turbines.

(2) Some discrepancies in magnitudes and variations with time between the results of fixed and flexible foundations in all the examined operating states were observed, indicating that the

soil effect cannot be neglected when analysing the seismic behaviour of wind turbines. By taking into account the nonlinear SSI and foundation flexibility, earthquake excitation induces more severe vibration on the tower resulting in more interactions between the rotor and turbulent wind. The tower-top fore-aft displacement is larger in comparison to that of the fixed foundations due to the effect of aerodynamic damping. Triggering an emergency shutdown does not mitigate the dynamic responses as expected for the flexible foundation under most examined wind conditions. Further consideration in the selection of appropriate operating state and dynamic control for a wind turbine subjected to a strong earthquake is required.

(3) The main contribution to the tower displacement comes from the 1st eigenmode of the support structure, indicating that the 2nd eigenmodes are less important. The shutdown decreases the response of the fixed case at the 1st fore-aft eigen-frequency during the strong shaking of the earthquake, while the relevant response of the flexible case is enhanced due to the shutdown. The observations imply that ignoring the soil effect may lead to misjudgements regarding the consequence of an emergency shutdown.

(4) The intersection between ground motion and inflow wind has significant influence on the seismic behaviour of the wind turbines. Therefore, it is required to examine both cases that interchange the horizontal components of an earthquake applied at the longitudinal and lateral directions for reducing the biases due to relative orientation with the wind direction.

Acknowledgements

The authors would like to acknowledge the financial support of National Natural Science Foundation of China (grant numbers: 51676131 and 51811530315) and Royal Society (grant number:

IEC\NSFC\170054). This project has received funding from the European Union's Horizon 2020 research and innovation programme under the Marie Skłodowska-Curie grant agreement no. 730888 (RESET) and European Regional Development Fund (ERDF), Interreg Atlantic Area (grant number: EAPA_344/2016). The first author is particularly grateful to Chinese Scholarship Council for funding his overseas study in the UK (grant number: 201708310149).

References

[1] GWEC. (2017). Global wind report 2017, Global Wind Energy Council report.

[2] China Earthquake Networks Center. http: //www.ceic.ac.cn/.

[3] Butt, U. A. & Ishihara, T. (2012). Seismic load evaluation of wind turbine support structures considering low structural damping and soil structure interaction. *European wind energy association annual event*, 16-19.

[4] Ishihara, T., & Sarwar, M. W. (2008, March). Numerical and theoretical study on seismic response of wind turbines. *In European wind energy conference and exhibition* (pp. 1-5).

[5] Dai, K., Huang, Y., Gong, C., Huang, Z., & Ren, X. (2015). Rapid seismic analysis methodology for in-service wind turbine towers. *Earthquake Engineering and Engineering Vibration*, 14(3), 539-548.

[6] Witcher, D. (2005). Seismic analysis of wind turbines in the time domain. *Wind Energy*, 8(1), 81-91.

[7] Wang, X., Yang, X., & Zeng, X. (2017). Seismic centrifuge modelling of suction bucket foundation for offshore wind turbine. *Renewable Energy*, 114, 1013-1022.

[8] Zheng, X. Y., Li, H., Rong, W., & Li, W. (2015). Joint earthquake and wave action on the monopile wind turbine foundation: An experimental study. *Marine Structures*, 44, 125-141.

[9] Yu, H., Zeng, X., & Lian, J. (2014). Seismic behaviour of offshore wind turbine with suction caisson foundation. *In Geo-Congress 2014: Geo-characterization and Modeling for Sustainability* (pp. 1206-1214).

[10] Prowell, I., Veletzos, M., Elgamal, A., & Restrepo, J. (2009). Experimental and numerical seismic response of a 65 kW wind turbine. *Journal of Earthquake Engineering*, 13(8), 1172-1190.

[11] Bazeos, N., Hatzigeorgiou, G. D., Hondros, I. D., Karamaneas, H., Karabalis, D. L., & Beskos, D. E. (2002). Static, seismic and stability analyses of a prototype wind turbine steel tower. *Engineering structures*, 24(8), 1015-1025.

[12] Lavassas, I., Nikolaidis, G., Zervas, P., Efthimiou, E., Doudoumis, I. N., & Baniotopoulos, C. C. (2003). Analysis and design of the prototype of a steel 1-MW wind turbine tower. *Engineering structures*, 25(8), 1097-1106.

[13] Hacıefendioğlu, K. (2012). Stochastic seismic response analysis of offshore wind turbine including fluid‐structure‐soil interaction. *The Structural Design of Tall and Special Buildings*, 21(12), 867-878.

[14] Ma, H., & Zhang, D. (2016). Seismic response of a prestressed concrete wind turbine tower. *International Journal of Civil Engineering*, 14(8), 561-571.

[15] Smith, V., & Mahmoud, H. (2016). Multihazard assessment of wind turbine towers under simultaneous application of wind, operation, and seismic loads. *Journal of Performance of Constructed Facilities*, 30(6), 04016043.

[16] Ritschel, U., Warnke, I., Kirchner, J., & Meussen, B. (2003). “Wind turbines and earthquakes.” *World Wind Energy Conference*, Cape Town, South Africa.

[17] Haenler, M., Ritschel, U., & Warnke, I. (2006). “Systematic modelling of wind turbine dynamics and earthquake loads on wind turbines.” *European Wind Energy Conference & Exhibition*,

Athens, Greece

[18] Zhao, X., & Maisser, P. (2006). Seismic response analysis of wind turbine towers including soil-structure interaction. *Proceedings of the Institution of Mechanical Engineers, Part K: Journal of Multi-body Dynamics*, 220(1), 53-61.

[19] Sapountzakis, E. J., Dikaros, I. C., Kampitsis, A. E., & Koroneou, A. D. (2015). Nonlinear response of wind turbines under wind and seismic excitations with soil–structure interaction. *Journal of Computational and Nonlinear Dynamics*, 10(4), 041007.

[20] Lloyd, G., & Hamburg, G. (2010). Guideline for the certification of wind turbines. July 1st.

[21] International Electrotechnical Commission. (2005). Wind turbines-part 1: design requirements. IEC61400-1 ed. 3.

[22] AWEA/ASCE. (2011). Recommended practice for compliance of large land-based wind turbine support structures, American Wind Energy Association and the American Society of Civil Engineers, Washington, USA.

[23] Prowell, I., Elgamal, A., Romanowitz, H., Duggan, J. E., & Jonkman, J. (2010). Earthquake response modeling for a parked and operating megawatt-scale wind turbine. *National Renewable Energy Laboratory, Technical Report No. NREL/TP-5000-48242*.

[24] Valamanesh, V., & Myers, A. T. (2014). Aerodynamic damping and seismic response of horizontal axis wind turbine towers. *Journal of Structural Engineering*, 140(11), 04014090.

[25] Santangelo, F., Failla, G., Santini, A., & Arena, F. (2016). Time-domain uncoupled analyses for seismic assessment of land-based wind turbines. *Engineering Structures*, 123, 275-299.

[26] Santangelo, F., Failla, G., Arena, F., & Ruzzo, C. (2018). On time-domain uncoupled analyses for offshore wind turbines under seismic loads. *Bulletin of Earthquake Engineering*, 16(2), 1007-1040.

[27] Katsanos, E. I., Sanz, A. A., Georgakis, C. T., & Thöns, S. (2017). Multi-hazard response analysis of a 5MW offshore wind turbine. *Procedia Engineering*, 199, 3206-3211.

[28] Prowell, I., Elgamal, A., & Jonkman, J. M. (2010). FAST simulation of wind turbine seismic response, *National Renewable Energy Laboratory, Technical Report No*. NREL/CP-500-46225.

[29] M. A. Asareh, I. Prowell, Seismic loading for FAST, *National Renewable Energy Laboratory, Technical Report No*. NREL/SR-500-53872.

[30] Asareh, M. A., Prowell, I., Volz, J., & Schonberg, W. (2016). A computational platform for considering the effects of aerodynamic and seismic load combination for utility scale horizontal axis wind turbines. *Earthquake Engineering and Engineering Vibration*, 15(1), 91-102.

[31] Jin, X., Liu, H., & Ju, W. (2014). Wind turbine seismic load analysis based on numerical calculation. *Strojniški vestnik-Journal of Mechanical Engineering*, 60(10), 638-648.

[32] Asareh, M. A., Schonberg, W., & Volz, J. (2016). Effects of seismic and aerodynamic load interaction on structural dynamic response of multi-megawatt utility scale horizontal axis wind turbines. *Renewable Energy*, 86, 49-58.

[33] Kim, D. H., Lee, S. G., & Lee, I. K. (2014). Seismic fragility analysis of 5 MW offshore wind turbine. *Renewable Energy*, 65, 250-256.

[34] Mo, R., Kang, H., Li, M., & Zhao, X. (2017). Seismic Fragility Analysis of Monopile Offshore Wind Turbines under Different Operational Conditions. *Energies*, 10(7), 1037.

[35] Alati, N., Failla, G., & Arena, F. (2015). Seismic analysis of offshore wind turbines on bottom-fixed support structures. *Phil. Trans. R. Soc. A*, 373(2035), 20140086.

[36] Huang, N. E., Shen, Z., Long, S. R., Wu, M. C., Shih, H. H., Zheng, Q., ... & Liu, H. H. (1998, March). The empirical mode decomposition and the Hilbert spectrum for nonlinear and non-stationary time series analysis. I*n Proceedings of the Royal Society of London A: mathematical,*

physical and engineering sciences (Vol. 454, No. 1971, pp. 903-995). The Royal Society.

[37] Jonkman, J., Butterfield, S., Musial, W., & Scott, G. (2009). Definition of a 5-MW reference wind turbine for offshore system development. *National Renewable Energy Laboratory, Technical Report No*. NREL/TP-500-38060.

[38] Jonkman, J., & Musial, W. (2010). Offshore code comparison collaboration (OC3) for IEA Wind Task 23 offshore wind technology and deployment. *National Renewable Energy Laboratory, Technical Report No*. NREL/TP-5000-48191.

[39] Harte, M., Basu, B. & Nielsen, S. R. (2012). Dynamic analysis of wind turbines including soil-structure interaction. Engineering Structures, 45, 509-518.

[40] Carswell, W., Johansson, J., Løvholt, F., Arwade, S. R., Madshus, C., DeGroot, D. J. & Myers, A. T. (2015). Foundation damping and the dynamics of offshore wind turbine monopiles. Renewable energy, 80, 724-736.

[41] Damgaard, M., Andersen, L. V. & Ibsen, L. B. (2015). Dynamic response sensitivity of an offshore wind turbine for varying subsoil conditions. Ocean engineering, 101, 227-234.

[42] Sun, C. (2018). Mitigation of offshore wind turbine responses under wind and wave loading: Considering soil effects and damage. Structural Control and Health Monitoring, 25(3), e2117.

[43] Passon, P. (2006). Memorandum: derivation and description of the soil-pile-interaction models. IEA-Annex XXIIII Subtask, 2.

[44] Yang, M., Ge, B., Li, W., & Zhu, B. (2016). Dimension effect on P-y model used for design of laterally loaded piles. Procedia engineering, 143, 598-606.

[45] Sahasakkul, W., Nguyen, H., & Sari, A. (2016, May). An improved methodology on design and analysis of offshore wind turbines supported by monopiles. In Offshore Technology Conference. Offshore Technology Conference.

[46] Bisoi, S., & Haldar, S. (2014). Dynamic analysis of offshore wind turbine in clay considering

soil–monopile–tower interaction. Soil Dynamics and Earthquake Engineering, 63, 19-35.

[47] Damgaard, M., Bayat, M., Andersen, L. V., & Ibsen, L. B. (2014). Assessment of the dynamic behaviour of saturated soil subjected to cyclic loading from offshore monopile wind turbine foundations. Computers and Geotechnics, 61, 116-126.

[48] Carswell, W., Arwade, S. R., DeGroot, D. J., & Lackner, M. A. (2015). Soil–structure reliability of offshore wind turbine monopile foundations. Wind energy, 18(3), 483-498.

[49] Álamo, G. M., Aznárez, J. J., Padrón, L. A., Martínez-Castro, A. E., Gallego, R., & Maeso, O. (2018). Dynamic soil-structure interaction in offshore wind turbines on monopiles in layered seabed based on real data. Ocean Engineering, 156, 14-24.

[50] DNV, D. N. V. (2013). Design of offshore wind turbine structures. Standard DNV-OSJ101, Det Norske Veritas AS (DNV).

[51] American Petroleum Institute(API). (2003). Petroleum and natural gas industries–Specific requirements for offshore structures–Part 4: Geotechnical and foundation design considerations. 19901-4: 2003 (E).

[52] Wind, G. L. (2005). Guideline for the certification of offshore wind turbines. Germanischer Lloyd Industrial Services GmbH.

[53] Makris, N., & Gazetas, G. (1992). Dynamic pile‐soil‐pile interaction. Part II: Lateral and seismic response. Earthquake engineering & structural dynamics, 21(2), 145-162.

[54] Jonkman, J. M., & Buhl Jr, M. L. (2005). FAST user's guide, *National Renewable Energy Laboratory, Technical Report No*. NREL/EL-500-38230.

[55] Pacific Earthquake Engineering Research (PEER) ground motion database. https://ngawest2.berkeley.edu/

[56] Jonkman, B. J. (2009). TurbSim user's guide: Version 1.50. *National Renewable Energy*

Laboratory, Technical Report No. NREL/TP-500-46198.

[57] Velarde, J. (2016). Design of monopile foundations to support the DTU 10 MW offshore wind turbine (Master's thesis, NTNU).

[58] Aranuvachapun, S. (1987). Parameters of Jonswap spectral model for surface gravity waves—II. Predictability from real data. Ocean engineering, 14(2), 101-115.

[59] Yang, Y., Ye, K., Li, C., Michailides, C., & Zhang, W. (2018). Dynamic behaviour of wind turbines influenced by aerodynamic damping and earthquake intensity. *Wind Energy*, 21(3).